Comparative Role of Neurotoxin-Associated Proteins in the Structural Stability and Endopeptidase Activity of Botulinum Neurotoxin Complex Types A and E[†]

Roshan V. Kukreja and Bal Ram Singh*

Botulinum Research Center, and Department of Chemistry and Biochemistry, University of Massachusetts Dartmouth, 285 Old Westport Road, North Dartmouth, Massachusetts 02747

Received August 4, 2007; Revised Manuscript Received September 28, 2007

ABSTRACT: Seven serotypes of botulinum neurotoxins, the most toxic substances known to mankind, are each produced by different strains of *Clostridium botulinum* along with a group of neurotoxin-associated proteins (NAPs). NAPs play a critical role in the toxicoinfection process of botulism in addition to their role in protecting the neurotoxin from proteolytic digestion in the GI tract as well as from adverse environmental conditions. In this study we have investigated the effect of temperature on the structural and functional stability of BoNT/A complex (BoNT/AC) and BoNT/E complex (BoNT/EC). Although the NAPs in the two complexes are quite different, both groups of NAPs activate the endopeptidase activities of their BoNTs without any need to reduce the disulfide bonds between light and heavy chains of respective BoNTs. BoNT/AC attains optimum enzyme activity at the physiological temperature of 37 °C whereas BoNT/EC is maximally active at 45 °C, and this is accompanied by conformational alterations in its polypeptide folding at this temperature, leading to favorable binding with its intracellular substrate, SNAP-25, and subsequent cleavage of the latter. BoNT/A in its complex form is found to be structurally more stable against temperature whereas BoNT/E in its complex form is functionally better protected against temperature. Based on the analysis of isolated NAPs we have observed that the structural stability of the BoNT/AC is contributed by the NAPs. In addition to the unique structural conditions in which the enzyme remains active, functional stability of botulinum neurotoxins against temperature plays a critical role in the survival of the agent in cooked food and in food-borne botulism.

Botulinum neurotoxin (BoNT[1]) is known to be the "most poisonous of all poisons" (*1*). The seven immunologically distinct serotypes of BoNT (A−G), each produced by various strains of *Clostridium botulinum*, act on the neuromuscular junction blocking the release of the neurotransmitter acetylcholine, thereby resulting in flaccid muscle paralysis (*2*, *3*). Although BoNT is the causative agent of the most dreaded food poisoning disease, botulism, it also remarkably serves as a powerful tool to treat an ever expanding list of medical conditions related to neuromuscular disorders (*4*, *5*).

Botulinum neurotoxin is a 150 kDa protein composed of a heavy chain (100 kDa) and a light chain (50 kDa) linked via disulfide bond(s) and noncovalent interactions. To produce its toxic effect, the toxin progresses through a series of well-defined steps that includes binding to receptors on the surface of cholinergic nerve endings mediated by the C-terminus of heavy chain, penetrating the plasma membrane by receptor-mediated endocytosis, penetrating the endosome by pH induced translocation, and finally acting in the cytosol to block neurotransmitter release (*6*, *7*). BoNTs possess Zn^{2+} endopeptidase activity against a select group of neuronal proteins involved in the exocytosis process, causing the blockage of acetylcholine release at the neuromuscular junction (*8*, *9*). BoNT serotypes A and E target the synaptosomal-associated protein of 25 kDa (SNAP-25). BoNT B, D, and F target the vesicle-associated membrane protein, synaptobrevin, also known as VAMP, and BoNT C cleaves syntaxin and SNAP-25 (*10*, *11*).

The most common source of botulism is by ingestion of food contaminated with spores of *C. botulinum* and preserved under anaerobic conditions that favor germination of spores and secretion of the neurotoxin (*12*). All BoNT serotypes are sensitive to the low pH and proteases of the gastric juice (*13*). The neurotoxins are associated with a group of nontoxic proteins called NAPs (neurotoxin-associated proteins) in the culture fluids to form large complexes which are designated progenitor toxins (*14*−*16*). NAPs play an important role in the stability of BoNTs in bacterial cultures under harsh environmental conditions and also play a critical role in protecting the BoNT from the acidity and proteases of the gastrointestinal tract (*17*, *18*). The oral toxicity of BoNT increases with incremental association of the neurotoxin with the NAPs (*17*). NAPs are also known to assist BoNT translocation across the intestinal mucosal layer (*19*, *20*). NAPs are apparently dissociated into the neurotoxin and the nontoxic components in the lymph after passing through the

[†] This work was supported by a DoD/Army Contract No. W911NF-06-1-0095 and by the National Institutes of Health through the New England Center of Excellence for Biodefense (Grant AI057159-01).

* Corresponding author. E-mail: bsingh@umassd.edu, telephone: 508-999-8588, fax: 508-999-8451.

[1] Abbreviations: BoNT, botulinum neurotoxin; BoNT/AC, botulinum neurotoxin type A complex; BoNT/EC, botulinum neurotoxin type E complex; LC, light chain; SNAP-25, synaptosomal-associated protein of 25 kDa; VAMP, vesicle-associated membrane protein; SNARE, soluble NSF attachment protein receptor; NAPs; neurotoxin-associated proteins; NaPB, sodium phosphate buffer; CD, circular dichroism; SDS-PAGE, sodium dodecyl sulfate−polyacrylamide gel electrophoresis.

10.1021/bi701564f CCC: $37.00
Published on Web 11/16/2007

small intestine or in alkaline conditions (*17*), implying no further roles of NAPs beyond translocation across the gut wall.

Because of the extreme toxicity and stability of BoNT in the presence of NAPs, BoNT complexes are on the top of the list of biological warfare agents (*21*). Ironically, it is the complex form of the BoNT that is used as therapeutic agent to treat several muscular disorders and in cosmetic applications (*22*), and NAPs may play a natural formulating agent for stable BoNT product. Furthermore, under certain conditions, such as direct injection of BoNT complex locally to treat neuromuscular disorders, NAPs could play further role in the action of the toxin by dramatically enhancing its endopeptidase activity (*23*, *18*).

BoNT produced in culture fluids with NAPs as complexes exist in three different forms. 19S referred to as the 'extra large' or LL complex, 16S complex referred to as 'large' or L toxin, and 12S known as M complex. BoNT/AC is known to exist in M, L, or LL forms. BoNTs B, C, D, and E complexes exist in M and L forms (*24*, *25*, *15*). BoNTs A, B, and E are responsible for majority of cases of human botulism (*26*), and hence any information obtained on the functional structure of BoNTs could provide an opportunity to design inhibitors and antidotes against human botulism.

Since much is known about the critical role of NAPs in the enhanced endopeptidase activity of BoNT/AC (*18*, *23*), and protection against proteases, heat, and acidity, a comparative study of the structure−function relationship of BoNT/AC with newly identified BoNT/EC (*25*) will provide a basis for deciphering the details of mechanism of their action at the molecular level which is important to BoNTs clinical applications and for developing antidotes against botulism. NAPs of BoNT/AC are quite different from that of BoNT/EC. An examination of their cumulative role in intact complex of BoNT/A and BoNT/E provides a unique opportunity to understand their structural and functional role in the neurotoxin action. Furthermore, BoNT/E targets the same intracellular substrate SNAP-25 as BoNT/A; thus, intense structural and biochemical analysis on BoNT/EC will provide an opportunity to compare with BoNT/AC especially for its relevance to binding and recognition of SNAP-25.

In this study, we have investigated the effect of temperature on the structural and functional stability of BoNT/A and E complexes. The results indicate that BoNT/AC is structurally more stable than BoNT/EC against temperature whereas BoNT/EC is functionally better protected against temperature in comparison to BoNT/AC. Functional stability of the botulinum complexes against temperature plays a critical role in the survival of the agent in cooked food and in food-borne botulism.

EXPERIMENTAL PROCEDURES

BoNT/AC and BoNT/EC Growth and Isolation. The procedure for the purification of BoNT/AC was adapted from previously established procedures (*27*). BoNT/EC was purified according to the method of Singh and Zhang (*25*).

Structural Analysis by Circular Dichroism. Circular dichroism (CD) spectra were recorded using a Jasco Model 715 spectropolarimeter (Jasco Inc., Easton, NJ). For far-UV CD measurements, spectra were recorded from 190 to 250 nm at a speed of 20 nm/min, with a response time of 8 s and a path length of 1 mm, at 20 °C. BoNT/AC and /EC samples dissolved in 10 mM NaPB (sodium phosphate buffer), pH 6.0, in the range of 0.2 to 0.3 mg/mL were used for far-UV CD measurements. A total of five scans were recorded and averaged to increase the signal-to-noise ratio. The final spectra were obtained after subtracting the buffer spectrum from the sample spectrum. Secondary structure elements were estimated according to previously established procedures (*28*). Near-UV CD spectra in the 250−340 nm region were recorded using a 10 mm cell containing 1−1.2 mg/mL protein dissolved in 10 mM NaPB, pH 6.0, at 20 °C. A scanning rate of 20 nm/min, response time of 8 s, and bandwidth of 1.0 mm were used. Final spectra, representing the average of at least five tracings, were corrected for the buffer spectrum.

Thermal Denaturation. Thermal denaturation of BoNT/AC and BoNT/EC was performed by increasing the temperature of the sample from 20 to 90 °C, with a slope of 2 °C/min, using a Jasco PTC-340W temperature control module. The far- and near-UV CD signals were monitored at 222 and 280 nm, respectively. All of the experiments were repeated at least three times using different preparations of the botulinum complexes. Thermodynamic parameters were calculated according to the methods described previously (*23*, *29*).

Tertiary Structural Analysis Using UV/vis Second Derivative Spectroscopy. Absorption spectra of BoNT/AC and BoNT/EC were recorded between 240 and 320 nm using a Jasco UV/vis spectrophotometer equipped with a temperature control module. The spectra were derivatized to the second order. The ratio of a (an arithmetic sum of the negative $d^2A/d\lambda^2$ at 285 nm and a positive $d^2A/d\lambda^2$ at 289 nm) and b (an arithmetic sum of the negative $d^2A/d\lambda^2$ at 291 nm and the positive $d^2A/d\lambda^2$ at 295 nm) was measured at different temperatures. The degree of tyrosine exposure for BoNT/AC was calculated according to the methods as described previously (*29*, *30*, *31*).

Fluorescence Spectroscopy. Fluorescence emission spectra of BoNT/AC and BoNT/EC were recorded using an ISS K2 fluorometer (Champaign, IL). The fluorescence spectra were recorded using an excitation wavelength of 295 nm. The excitation and emission slit widths were set to 8 nm. In order to minimize the inner filter effect, the sample concentration was fixed such that the absorbance at 295 nm was less than 0.1.

Enzymatic Activity Assay. The endopeptidase activity of BoNT/AC and BoNT/EC was estimated using their intracellular target protein, recombinant His-tagged rat SNAP-25a, as substrate. The temperature effect on the endopeptidase activity of the botulinum complexes was examined by incubating 6 μM SNAP-25 with 200 nM BoNT/AC, and 6.4 μM SNAP-25 with 200 nM BoNT/EC, at the designated temperature for 30 min in an assay buffer (50 mM Tris, 10 mM sodium phosphate, 300 mM NaCl, 2 mM $MgCl_2$, 0.3 mM $CaCl_2$, and 0.1% NaN_3, pH 7.6). The cleavage reaction was terminated by addition of SDS-PAGE sample buffer, and the samples were then separated on 4−20% sodium dodecyl sulfate−polyacrylamide gel electrophoresis (SDS-PAGE). The electrophoresis was run using a Mini Protean III system from BioRad (Hercules, CA) at 25 °C under a constant voltage of 200 V. The bands on the gel were visualized by Coomassie blue staining. The amount of

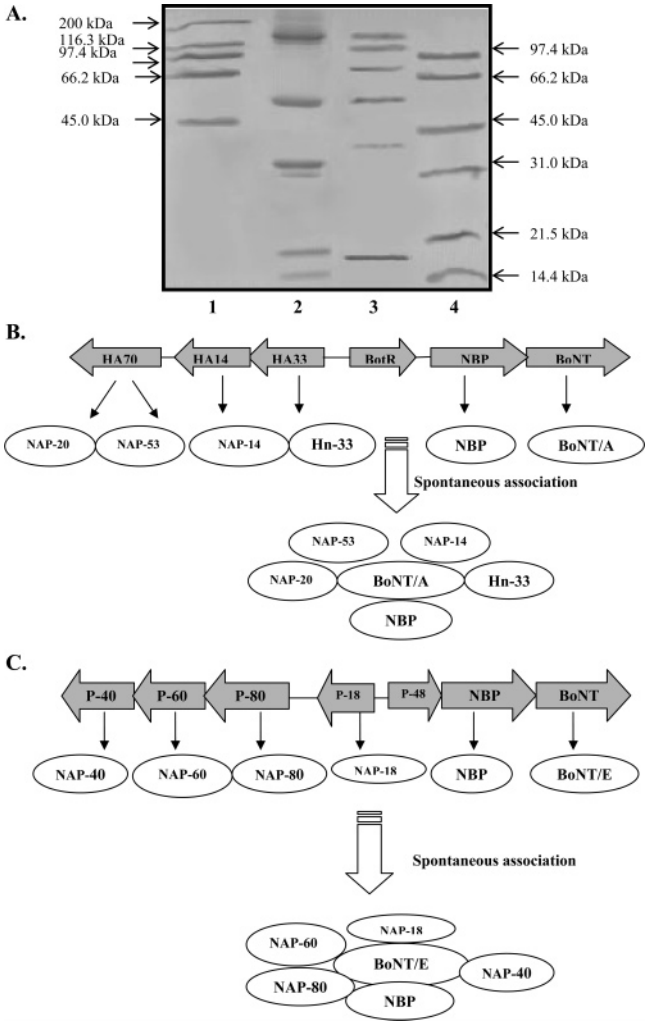

FIGURE 1: A, SDS-PAGE analysis of BoNT/AC and BoNT/EC under nonreducing conditions visualized by Coomassie blue staining. Lane 1: High molecular mass protein marker; lane 2: BoNT/AC; lane 3: BoNT/EC; lane 4: low molecular mass protein marker. B, Schematic diagram showing the genomic organization of *C. botulinum* type A (*20*) and their expressed proteins in forming BoNT/AC. C, Schematic diagram showing the genomic organization of *C. botulinum* type E (*17*) and their expressed proteins in forming BoNT/EC.

uncleaved SNAP-25 was scanned on a GEL LOGIC 100 Image system and analyzed and quantified using the Kodak Image analysis software (Eastman Kodak Co., Rochester, NY). The percentage of cleavage was calculated by comparing the density of the uncleaved SNAP-25 band to that of the control SNAP-25.

RESULTS

BoNT and NAPs in BoNT /AC and BoNT/EC. Freshly prepared BoNT/AC and BoNT/EC each exhibited six Coomassie blue stained protein bands when analyzed on a 4−20% SDS-PAGE gel under nonreducing conditions (Figure 1A). For BoNT/AC the protein bands correspond to 145 (BoNT/A), 120 (NBP: neurotoxin binding protein), 53 (NAP-53), 33 (Hn-33), 20 (NAP-20), and 14 kDa (NAP-14) (*23*). For BoNT/EC, the protein band correspond to 138 (BoNT/E), 118 (NBP), 80 (NAP-80), 60 (NAP-60), 40 (NAP-40), and 18 kDa (NAP-18) (*17*, *25*, *32*). The assignments of bands observed on SDS-PAGE gels are based on previous biochemical and genetic analysis of BoNT/AC and

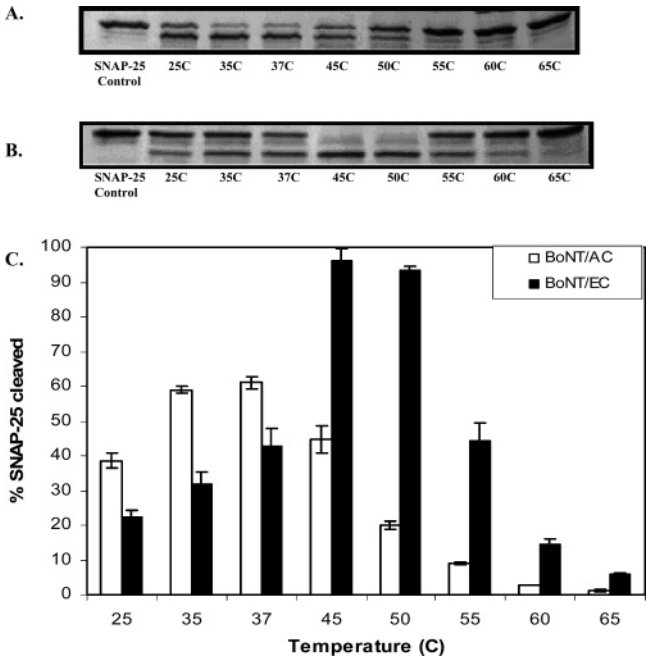

FIGURE 2: A, SDS-PAGE analysis of endopeptidase activity of BoNT/AC at different temperatures using SNAP-25 as its substrate. SNAP-25 (6 μM) was incubated with 200 nM BoNT/AC at varying temperatures for 30 min. B, SDS-PAGE analysis of endopeptidase activity of BoNT/EC at different temperatures using SNAP-25 as its substrate. SNAP-25 (6.4 μM) was incubated with 200 nM BoNT/EC at varying temperatures for 30 min. C, Endopeptidase activity of BoNT/AC and BoNT/EC as a function of temperature. Cleavage percentage of SNAP-25 by BoNT/AC and BoNT/EC was monitored at varying temperatures. The error bars represent the standard deviation of three independent experiments.

BoNT/EC (*23*, *32*, *17*, *25*, *31*, Chang and Singh, unpublished results). A schematic model of BoNT/AC and BoNT/EC genes and their expressed proteins is shown in Figures 1B and 1C, respectively.

Heat-Activated Zn^{2+} Endopeptidase Activity of BoNT/A and BoNT/E Neurotoxin Complex. The substrates for the zinc endopeptidase activity of BoNTs are the components of the cellular secretory machinery. The 25 kDa synaptosomal-associated protein (SNAP-25) is the intracellular substrate for BoNT/A and BoNT/E. To investigate the functional stability of BoNT/AC and BoNT/EC against temperature, we determined their endopeptidase activity on SNAP-25 as a function of temperature. It was observed that the endopeptidase activity of BoNT/AC at 200 nM concentration reaches a maximum at 37 °C (Figure 2A), as revealed by the 61.0 ± 1.9% cleavage of SNAP-25 (Figure 2C). As the temperature was further increased, it was observed that BoNT/AC retained 33% of the optimum enzymatic activity at 50 °C, and beyond this temperature it displayed only residual activity (Figure 2C). BoNT/EC at 200 nM, on the other hand, was found to have optimum enzymatic activity at 45 °C (Figure 2B), where it cleaves 96.1 ± 3.6% SNAP-25 as seen in Figure 2C. BoNT/EC retained significant activity (42% of the optimum enzyme activity) even at a high temperature of 55 °C, and beyond this temperature it retained only residual activity. To confirm that the optimum activities of BoNT/AC and BoNT/EC were not higher than 37 °C, or lower than 45 °C, respectively, we monitored the endopeptidase activity of both BoNT/AC and BoNT/EC at an interim temperature of 40 °C and observed that the activity of BoNT/

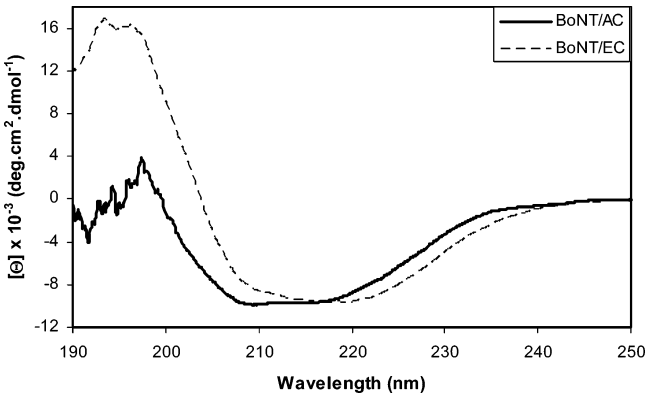

FIGURE 3: Far-UV CD spectra of BoNT/AC and BoNT/EC recorded at 20 °C in 10 mM sodium phosphate buffer, pH 6.0. Spectral recording was carried out at a speed of 20 nm/min and with a response time of 8 s. Baseline corresponding to the buffer solution was subtracted.

Table 1: Secondary Structure Estimation of BoNT/A and BoNT/E Complexes

protein	α-helix (%)	β-sheets (%)	β-turns (%)	random (%)
BoNT/AC	12.7 ± 1.6	49.8 ± 3.5	9.1 ± 2.9	28.5 ± 0.6
BoNT/EC	32.4 ± 2.9	41.8 ± 6.2	8.6 ± 1.7	17.3 ± 2.7

AC remained highest at 37 °C and that of BoNT/EC was optimum at 45 °C.

In an effort to confirm that SNAP-25 itself was not degrading at such high temperatures, BoNT/AC and BoNT/EC alone were heated to different temperatures and then added to SNAP-25. The reaction was allowed to proceed at 37 °C for 30 min. This experiment confirmed that BoNT/AC and BoNT/EC are optimally active at 37 °C and 45 °C, respectively, and that BoNT/EC retains 40% enzyme activity even at a high temperature of 55 °C (data not shown).

Temperature-Induced Conformational Transitions in BoNT/A and BoNT/E Neurotoxin Complexes. To elucidate the structural basis of their differential temperature profile of enzyme activity, we first analyzed the secondary structures of BoNT/AC and BoNT/EC by far-UV CD. As seen in Figure 3, significant difference in the far-UV CD signal at 222 nm was observed for the two complexes. BoNT/EC was found to have more α-helical structure than BoNT/AC as indicated by the secondary structure estimation of the two proteins (Table 1). In addition, the far-UV CD signal at 208 nm indicated that BoNT/AC possesses more random coil structure than BoNT/EC. This suggests different conformations for the two complexes, as would be expected from their different composition of proteins.

To further distinguish the molecular folding patterns of the two complexes, thermal denaturation analysis was carried out. Upon heating, BoNT/AC exhibited a sharp typical unfolding transition with melting temperature (T_m) of around 75 °C (Figure 4). BoNT/EC, on the other hand, exhibited a significantly different transition curve with a smooth but slow unfolding transition. The T_m for BoNT/EC unfolding was 63 °C, indicating a relatively unstable structure (Figure 4). Comparison of the temperature-induced unfolding profile of BoNT/AC and BoNT/EC indicated that BoNT/AC displays an abrupt cooperative pattern of unfolding which starts from 70 °C and ends at 80 °C, indicative of a two-state (N↔U) unfolding whereas BoNT/EC exhibits a gradual unfolding

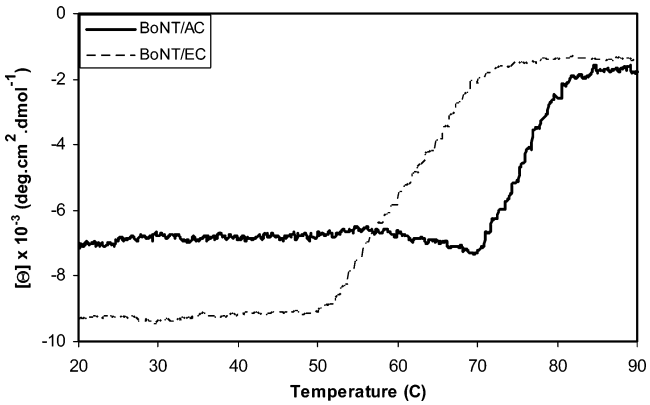

FIGURE 4: Thermal denaturation profile of BoNT/AC and BoNT/EC monitored by recording the CD signal at 222 nm. Sample was heated from 20 to 90 °C, at a rate of 2 °C/min.

Table 2: Thermodynamic Parameters for the Temperature-Induced Denaturation of BoNT/AC and BoNT/EC Based on the CD Signal at 222 nm

protein	Δ*H* (kJ/mol)	Δ*S* (J/K.mol)	Δ*G* (kJ/mol)	T_m (°C)
BoNT/AC	351.3 ± 18.4	995.1 ± 51.9	51.3 ± 3.8	75.6 ± 1.4
BoNT/EC	115.3 ± 5.3	337.9 ± 15.7	14.6 ± 0.8	63.2 ± 0.8

wherein it undergoes a broad and slow unfolding transition from 48 °C to 75 °C indicative of a noncooperative unfolding. These observations suggest that BoNT/EC is conformationally less stable than BoNT/AC.

Temperature-induced unfolding of BoNT/AC and BoNT/EC resulted in aggregate formation, as observed for many large proteins (*24*). To estimate thermodynamic parameters of protein unfolding, it is assumed that the process occurs as a single reversible phenomenon. Therefore, it was not appropriate to calculate true thermodynamic parameters (Δ*G*, Δ*S*, and Δ*H*) (*29*, *35*). Calculation of pseudo-thermodynamic parameters revealed that Δ*H*, Δ*S*, and Δ*G* values for BoNT/AC were approximately three times higher than those for BoNT/EC (Table 2). These results indicate a higher degree of flexibility in the polypeptide folding of BoNT/EC in comparison to BoNT/AC.

To understand the structural basis of differential enzyme activities of BoNT/A in its purified and complex forms, we analyzed the secondary structures of BoNT/A in complex and purified forms and the structure of NAPs that were isolated from BoNT/AC, by far-UV CD. As seen in Figure 5, BoNT/AC exhibits a different spectral profile as compared to that of pure BoNT/A. Spectral analysis revealed that BoNT/A has 43% more α-helical structure than BoNT/AC or isolated NAPs. While it has not been possible to separately monitor BoNT/A structure within the complex, the dramatic difference in the protein secondary structure of BoNT/A in its purified and complex forms suggests that the interaction with NAPs leads to substantial changes in BoNT/A. To further investigate differential molecular folding profile of BoNT/A in its complex and purified forms, we carried out temperature-induced unfolding of the proteins. BoNT/AC exhibited a typical unfolding transition with a melting temperature (T_m) of 75 °C. NAPs unfolded with T_m of 72 °C whereas, T_m for pure BoNT/A unfolding was found to be 54 °C (Figure 5, inset). This suggests that interaction of NAPs with the neurotoxin in the complex enhances its structural stability against temperature. Taken together, these

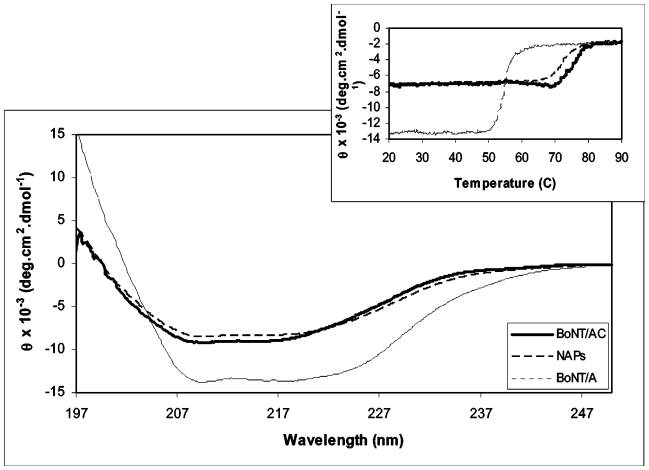

FIGURE 5: Far-UV CD spectra of BoNT/AC, NAPs, and BoNT/A recorded at 20 °C in 10 mM sodium phosphate buffer, pH 6.0. Spectral recording was carried out at a speed of 20 nm/min and with a response time of 8 s. Baseline corresponding to the buffer solution was subtracted. Inset: Thermal denaturation profile BoNT/AC (−), NAPs (- - -), and BoNT/A (·····) monitored by recording the CD signal at 222 nm. Sample was heated from 20 to 90 °C, at a rate of 2 °C/min.

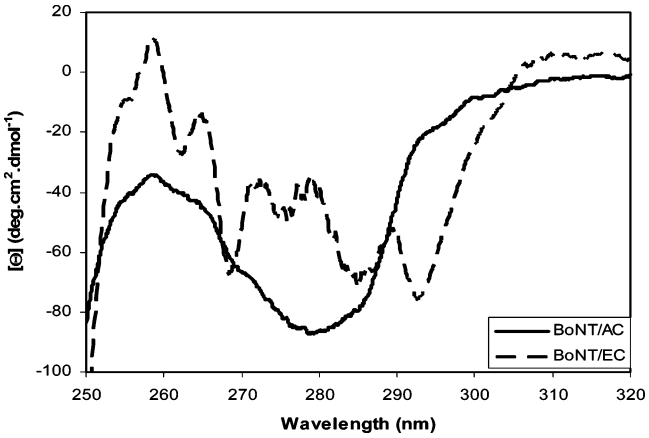

FIGURE 6: Near-UV CD spectrum of BoNT/AC and BoNT/EC recorded at 20 °C in 10 mM sodium phosphate buffer, pH 6.0. Spectral recording was carried out from 250 to 320 nm at a speed of 20 nm /min and with a response time of 8 s.

data suggest that the endopeptidase activity of BoNT/A in the complex where its disulfide bond remains intact may reflect an enzymatically active conformational state which may be similar to the enzymatically active molten globule or PRIME conformation we have observed previously (*23*, *36*).

Near-UV CD technique is used to probe tertiary structural changes in proteins that affect the environment of aromatic amino acid residues (*37*, *38*). The near-UV CD spectra of the two complexes are dramatically distinct as seen in Figure 6. The near-UV CD spectrum of BoNT/AC shows a major negative band at 280 nm (Figure 6), corresponding to asymmetry around Tyr residues. The shoulder at 286 nm corresponds to Trp residues (*39*). The shoulder observed at 265 nm can be attributed to Phe residues. BoNT/EC, on the other hand, displayed a strikingly different near-UV CD spectrum (Figure 6). The band observed at 292 nm can be assigned to the ^1L_b transition of Trp residues (*29*, *23*), while the band observed at 286 nm corresponds to the ^1L_a transition of Trp residues (*40*). The near-UV CD spectrum of BoNT/EC also shows major negative peaks at 261 and 269 nm which can be ascribed to Phe residues (*29*). A shoulder at 278 nm can be attributed to the Tyr residues. A strong near-UV CD signal at 280 nm for BoNT/AC compared to BoNT/EC indicates that Tyr residues in BoNT/AC are deeply buried in the protein matrix while BoNT/EC has a looser hydrophobic core containing Tyr residues.

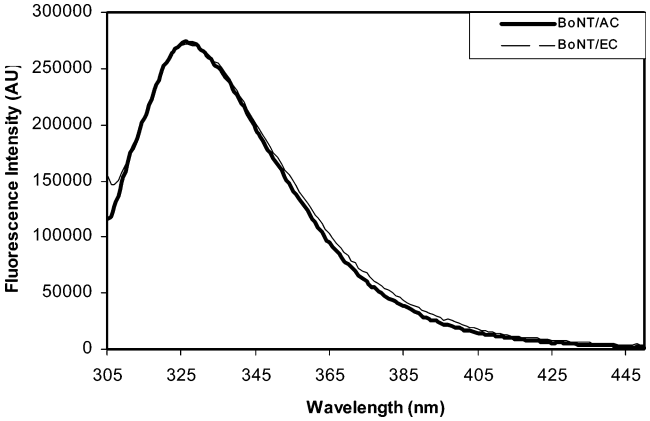

FIGURE 7: Fluorescence emission spectra BoNT/AC and BoNT/EC dissolved in 10 mM sodium phosphate buffer, maintained at pH 6.0. Spectral recordings were carried out at room temperature. Excitation wavelength was set at 295 nm. The absorbance at 295 nm was less than 0.1 for the samples. Excitation and emission slit widths were set at 8 nm.

Results obtained when the thermally induced unfolding of BoNT/AC and BoNT/EC was examined by monitoring the CD signal at 280 nm as a function of temperature were the same as those seen when the unfolding was monitored at 222 nm (data not shown). The lower T_m observed for BoNT/EC again indicated a relatively unstable structure.

Comparative tertiary structural changes in BoNT/AC and BoNT/EC as a function of temperature were also analyzed by monitoring the topography of Tyr residues using UV second derivative spectroscopy, and Trp residues using fluorescence emission spectroscopy. Figure 7 shows the fluorescence emission spectra of BoNT/AC and BoNT/EC obtained between 310 and 450 nm after exciting the samples at 295 nm at 25 °C. Both BoNT/AC and BoNT/EC exhibited identical scans with emission maximum at 327 nm. The excitation at 295 nm selectively excites Trp residues. The significantly blue-shifted emission maximum of Trp fluorescence {fluorescence emission maximum of free Trp is at around 350 nm (*39*)} in both BoNT/AC and BoNT/EC suggest that fluorescent Trp residues in the proteins are located in the hydrophobic environment of protein matrix and that both BoNT/AC and /EC have identical topography around Trp residues at room temperature.

The second derivative UV absorption spectrum of BoNT/AC and BoNT/EC at 25 °C is shown in Figure 8A and 8B, respectively. The spectral region of interest for the determination of exposed Tyr residues is 280−300 nm. The spectra of both the proteins exhibited the typical second derivative negative and positive peaks of proteins at 285, 289, 292, and 295 nm (*41*, *40*). Even though the peak positions in the second derivative spectrum of the two complexes remained the same, there was significant difference in their a/b ratios indicating different topography around Tyr residues in the proteins (Figure 8C). The ratio of a (an arithmetic sum of the negative $d^2A/d\lambda^2$ at 285 nm and a

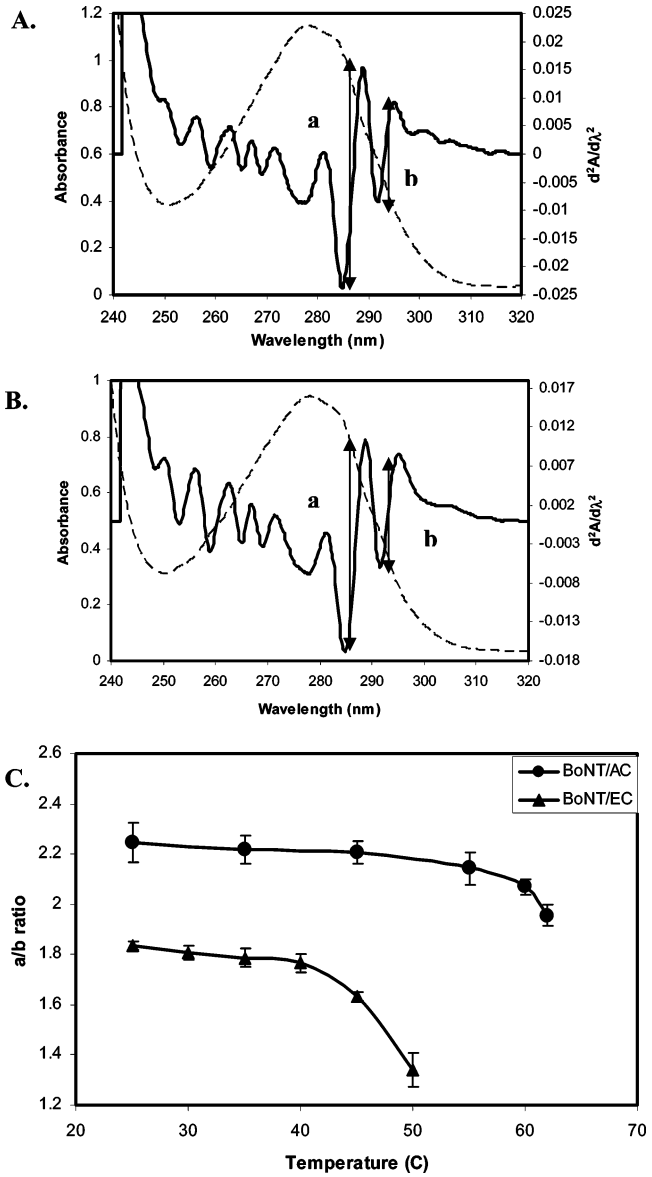

FIGURE 8: A, Absorption (---) and second derivative (−) spectra of BoNT/AC dissolved in 10 mM sodium posphate buffer, pH 6.0 at 25 °C. B, Absorption (---) and second derivative spectra (−) of BoNT/EC dissolved in 10 mM sodium phosphate buffer, pH 6.0 at 25 °C. C, Effect of increasing temperature on the second derivative ratio (a/b) of BoNT/AC (●) and BoNT/EC (▲) dissolved in 10 mM NaPB, pH 6.0.

positive $d^2A/d\lambda^2$ at 289 nm) and b (an arithmetic sum of the negative $d^2A/d\lambda^2$ at 292 nm and the positive $d^2A/d\lambda^2$ at 295 nm) for BoNT/AC and BoNT/EC at 25 °C was 2.25 ± 0.18 and 1.83 ± 0.02, respectively (Figure 8C).

To probe the effect of temperature on the tertiary structural changes, second derivative absorption spectra were obtained at different temperatures (25−65 °C). The a/b ratio was determined at each of these temperatures to determine the change in exposure of Tyr residues in the proteins with temperature. It was observed that with increasing temperatures, the a/b ratio for the 2 complexes, decreased suggesting a lower exposure of Tyr residues (*42*). The a/b ratios of BoNT/AC at 25 °C and 62 °C were 2.25 ± 0.08 and 1.96 ± 0.04, respectively, reflecting a decrease of 13% in the a/b ratio at 62 °C from that at 25 °C (Figure 8C) whereas for BoNT/EC, the a/b ratios at 25 °C and 50 °C were 1.83 ± 0.02 and 1.34 ± 0.06, respectively, reflecting a decrease of 27% (Figure 8C). It was difficult to accurately measure the peak ratios beyond 62 °C and 50 °C for BoNT/AC and BoNT/EC, respectively, because of noise in the spectrum which could have resulted from aggregation of the proteins upon further heating.

Estimation of degree of Tyr exposure (carried out as described previously; *36*) upon complete denaturation of BoNT/AC with 6 M guanidine.HCl (30 min at 25 °C) revealed that about 94% of Tyr residues of BoNT/AC were exposed to polar solvent environment (data not shown). Degree of Tyr exposure could not be determined for BoNT/EC, as the amino acid sequence for the entire large complex is not yet known.

DISCUSSION

Among the unique characteristics of BoNTs (*43*), its novel endopeptidase activity is the most critical and defining feature of these macromolecules (*44*). The endopeptidase activity of the intact toxin is expressed only under the condition when the disulfide bond between its light and heavy chain is reduced, or the light chain is separated from the heavy chain. These features are consistent with the mode of action in which the disulfide bond between the chains is reduced during the translocation process and the separated light chain is available in the cytosol of nerve cells (*21*). Another unique characteristic of BoNTs is their complex forms consisting of BoNT and NAPs. The NAPs and BoNTs are not only genetically encoded as gene clusters and physically associated but are functionally involved in the protection against low pH and proteases in the GI tract, translocation across the gut wall, and dramatic activation of the endopeptidase activity. The role of NAPs in the activation of the endopeptidase activity is particularly noteworthy for further examination, as the presence NAPs in BoNT complex results in activated endopeptidase without the need to reduce the disulfide bond between the light and heavy chain. Since we have obtained two entirely different groups of NAPs in BoNT/AC and BoNT/EC, examination of variation in endopeptidase activity with temperature-induced conformational states of these complexes is expected to reveal a common mechanism of enhancement of endopeptidase activity by NAPs.

Examination of the biological activity of BoNT/AC revealed that it acquires optimum activity at the physiological temperature of 37 °C under conditions where the disulfide bond between the light chain and the heavy chains was not reduced (Figure 2A and 2C), which is a behavior similar to that of the reduced form of BoNT/A neurotoxin and the light chain of BoNT/A (*36*, *45*). This enhancement in the endopeptidase activity of BoNT/A in the complex has been attributed to its direct interaction with NAPs leading BoNT/A to adopt a structurally active state similar to that of reduced BoNT/A (*23*). At 37 °C, BoNT/A under reducing conditions exists in a molten globule conformation and that is the enzymatically active structure (*45*). Recently we have also shown that the endopeptidase moiety of BoNT/A (the light chain) acquires a novel PRIME conformation at 37 °C and exhibits maximum endopeptidase activity against its intracellular substrate, SNAP-25, at this temperature (*36*). Our observation of the optimal endopeptidase activity of BoNT/AC at 37 °C reinforces the hypothesis of a conformational

alteration in BoNT/A upon its interaction with NAPs in the complex. This altered conformation of BoNT/A in the complex, similar to the molten globule conformation of reduced BoNT/A or the PRIME conformation of the light chain of BoNT/A at physiological temperature, may facilitate its favorable interaction with SNAP-25, leading to the optimal cleavage of the latter at this temperature, even under conditions which keep the disulfide bond between the light and heavy chains of BoNT/A intact.

This implication of a substantial functional role of NAPs requires further experimental evidence to provide a confirmed mechanism of the enhanced enzyme activity. At a minimum, these results suggest the substantial role of NAPs in the critical endopeptidase activity of BoNT, which may even have relevance to the biological activity of BoNT *in vivo*. While the toxicoinfection process of botulism assumes separation of the NAPs from BoNT before reaching the nerve cell, injection of BoNT/A complex for therapeutic or cosmetic use does not separate the two components. Furthermore, currently it is not known what role the toxin plays inside the bacterial cell or in the native ecologically conditions of *C. botulinum*. An activated form of the endopeptidase complex may have a critical role under those conditions.

Interestingly, BoNT/EC, under nonreducing conditions, was found to exhibit optimum enzyme activity at 45 °C (Figure 2B) and displays a 2.3-fold higher activity at this temperature than that at 37 °C (Figure 2C). We have observed that the reduced form of single chain BoNT/E is maximally active at 45 °C (Kukreja and Singh, unpublished results). Because the purified single chain BoNT/E under nonreducing conditions is enzymatically inactive (*18*), it can be concluded that the enhanced endopeptidase activity of BoNT/E in the complex (wherein it exists in the nonreduced single chain form) is likely to result from its interaction with the NAPs. This interaction must introduce specific changes in BoNT/E to adapt a structurally active state similar to that of the reduced form of single chain BoNT/E, a phenomenon similar to the one observed in BoNT/AC.

BoNT/AC is composed of six NAPs including Hn-33. Hn-33 makes up the largest fraction of the NAPs in BoNT/AC (*46*) and strongly protects the toxin against proteases (*47*). The X-ray crystallographic structure of BoNT/A indicates that the active site is buried 20−24 Å deep in the protein matrix and is partially shielded by a belt from the N-terminal domain of the heavy chain involved in disulfide bond formation and that the reduction of the disulfide bond exposes the active site (*48*). Recently it has been proposed that the interaction of Hn-33 with BoNT/A in the complex exposes the enzyme active site without the need of opening the belt, leading to its enhanced enzyme activity, and that Hn-33 mimics the effect of all NAPS in enhancing the endopeptidase activity of BoNT/A (*18*). Hn-33 from BoNT/AC also enhanced the endopeptidase activity of BoNT/E, suggesting a common structural motif of BoNT serotypes for Hn-33 (*18*). However, our report wherein BoNT/EC that is devoid of Hn-33 also displays enzyme activity under nonreducing conditions (∼42% at 37 °C, and 96% at 45 °C) (Figure 2C) suggests that the interaction of BoNT/E with the NAPs present in BoNT/EC is sufficient to alter the structure of the neurotoxin where it conforms to a structurally active state similar to that of the reduced form of BoNT/E. However, the efficiency of cleavage of SNAP-25 by BoNT/EC is less than that of BoNT/AC at 37 °C (BoNT/AC displays 32% higher endopeptidase activity than that of BoNT/EC at 37 °C; Figure 2C). Higher toxicity of BoNT/A in comparison to BoNT/E may in part be reflected by the fact that BoNT/A in its complex form is more enzymatically active at the physiological temperature of 37 °C as compared to BoNT/E in the complex form.

The effect of temperature on the polypeptide folding of BoNT/AC and BoNT/EC was examined by monitoring CD signals at 222 and 280 nm as a function of temperature. The unfolding curves of both the complexes obtained from CD recordings in the far- and near-UV regions coincide and indicate that both the secondary and tertiary structures for both the complexes unfolded simultaneously and the T_m for the unfolding was 75 °C and 63 °C for BoNT/AC and BoNT/EC, respectively. However, the temperature denaturation profile of BoNT/EC reveals that the unfolding transitions in this protein occur over a significantly broader temperature range than those of BoNT/AC, suggesting a less cooperative unfolding of BoNT/EC which would be consistent with a nonrigid structure. The lower T_m value observed for BoNT/EC indicates that it is conformationally less stable than BoNT/AC (Figure 4).

Thermal denaturation of proteins provides key thermodynamic information about the stability of proteins. The free energy change (ΔG) for the unfolding of BoNT/EC was 70% higher than that of BoNT/AC, suggesting that BoNT/EC is less heat stable than BoNT/AC. This observation is further supported by both a smaller ΔH and expected higher entropy (as reflected by smaller ΔS in Table 2). The 3-fold higher values for ΔH and ΔG for BoNT/AC compared to BoNT/EC indicate that the unfolding transition for BoNT/EC is more spontaneous compared to BoNT/AC. These results indicate a higher degree of flexibility in the polypeptide folding of BoNT/EC.

The effect of temperature on the solvent accessibility of tyrosyl residues of BoNT/AC and BoNT/EC were also examined by means of UV second derivative spectroscopy in the near-ultraviolet region. With increasing temperatures, a marked decrease in the a/b ratios of BoNT/AC and BoNT/EC with T_m of around 62 °C and 45 °C, respectively (Figure 8C), suggesting lower exposure of tyrosine residues upon heating. A significant change in the polypeptide folding is likely to affect the degree of tyrosine residues exposed to the protein surface (*42*, *36*). These results suggest that significant changes in the polypeptide folding of BoNT/EC occur upon heating, and that at a temperature of around 45 °C, it exists in a conformational state that is different from the native state (25 °C) or from the conformational state that is at the physiological temperature of 37 °C. Interestingly, it is at this temperature that BoNT/EC exhibits optimum enzyme activity (Figure 2C). This change in the conformation of BoNT/EC at 45 °C may be responsible for its optimum enzyme activity at this temperature. It is possible that at this temperature the interactions of BoNT/E with the NAPs in the complex may be favorable to bring the enzyme active site close to the substrate cleavage site which in turn leads to maximum cleavage of SNAP-25 at this temperature as compared to that at 37 °C. The topography of Tyr residues is known to play an important role in the toxicity of BoNT/E, since the modification of 10−12 tyrosine residues in BoNT/E by tetranitromethane abolished the toxicity (*49*).

The two complexes (BoNT/AC and BoNT/EC) have significant differences in their protein components, composition, and conformation reflected by secondary structure analysis, near-UV CD spectra, and temperature denaturation pattern of secondary and tertiary structures. However, NAPs seem to play a similar structural and functional role in protecting the toxin and enhancing its endopeptidase activity, suggesting the presence of specific interactions between the two components (BoNT and NAPs) of BoNT complexes.

It is notable that we carried out the denaturation of BoNT/AC and BoNT/EC at pH 6.0, which is similar to the pH of bacterial cultures where the toxin is released. Examination of the stability of the two complexes at that pH is closer to the native conditions. We carried out the enzyme activity at a pH closer to the physiological condition to relate it to any biological relevance it may have to humans or animals. We have tested the temperature profile of the enzymatic activity at pH 6.0 and 7.6, which showed an identical profile (*36*). We have also carried out CD spectral analysis as well as a denaturation profile of BoNT/AC and BoNT/EC at both pHs and observed identical spectral profiles (data not shown).

In summary, we have demonstrated the following: (i) BoNT/A and BoNT/E in their complex forms are enzymatically active under nonreducing conditions. BoNT/AC under nonreducing conditions attains optimum activity at the physiological temperature of 37 °C whereas BoNT/EC under nonreducing conditions achieves maximum endopeptidase activity at 45 °C. (ii) BoNT/EC undergoes conformational alterations in its polypeptide folding at 45 °C, and this may result in its favorable binding with the substrate leading to maximum cleavage of the latter. (iii) Because of the direct interaction with NAPs, BoNT/A and E in their respective complex forms may conform to a structurally active state which is similar to that of the reduced BoNT/A and BoNT/E, respectively, leading their enhanced endopeptidase activity. (iv) BoNT/AC is structurally more stable while BoNT/EC is functionally more stable against temperature.

REFERENCES

1. Lamanna, C. (1959) The most poisonous poison, *Science 130*, 763−772.
2. Singh, B. R. (2000) Intimate details of the most poisonous poison, *Nat. Struct. Biol. 7*, 617−619.
3. Coffield, J. A. (2003) Botulinum neurotoxin: the neuromuscular junction revisited, *Crict. Rev. Neurobiol. 15*, 175−195.
4. Klien, A. W. (2004) The therapeutic potential of botulinum toxin, *Dermatol. Surg. 30*, 452−455.
5. Bhidayasiri, R., and Truong, D. D. (2005) Expanding use of botulinum toxin, *J. Neurol. Sci. 235*, 1−9.
6. Montecucco, C., and Schiavo, G. (1995) Structure and function of tetanus and botulinum neurotoxins, *Q. Rev. Biophys. 28*, 423−472.
7. Dressler, D., and Saberi, F. A. (2005) Botulinum toxin: mechanisms of action, *Eur. Neurol. 53*, 3−9.
8. Tonello, F., Morante, S., Rossetto, O., Schiavo, G., and Montecucco, C. (1996) Tetanus and botulinum neurotoxins, *Adv. Exp. Med. Biol. 389*, 251−260.
9. Swaminathan, S., Eswaramoorthy, S., and Kumaran, D. (2004) Structure and enzymatic activity of botulinum neurotoxins, *Movement Disorders 19*, S17−S22.
10. Li, L., and Singh, B. R. (1999) Structure-function relationship of clostridial neurotoxins, *J. Toxicol., Toxin Rev. 18*, 95−112.
11. Chaddock, J. A., and Marks, P. M. H. (2006) Clostridial neurotoxins: structure-function led design of new therapeutics, *Cell. Mol. Life Sci. 63*, 540−51.
12. Chen, F., Kuziemko, G. M., and Stevens, R. C. (1998) Biophysical characterization of the stability of the 150 kDa botulinum toxin, the nontoxic component, and the 900-kDa botulinum toxin complex species, *Infect. Immun. 66*, 2420−2425.
13. Humeau, Y., Doussau, Grant, F., N. J., and Poulain, B. (2000) How botulinum and tetanus neurotoxins block neurotransmitter release, *Biochimie 82*, 427−46.
14. Inoue, K., Fujinaga, Y., Watanabe, T., Ohyama, T., Takeshi, K., Moriishi, K., Nakajima, H., and Oguma, K. (1996) Molecular composition of *Clostridium botulinum* type A progenitor toxins, *Infect. Immun. 64*, 1589−1594.
15. Singh, B. R. (2002) in *Scientific and Therapeutic Aspects of Botulinum Toxin* (Brin, M. F., Jankovic, J., and Hallet, M., Eds.) pp 75−88, Lipincott Williams and Wilkins, Philadelphia.
16. Ting, P. T., and Freiman, A. (2004) The story of clostridium botulinum: from food poisoning to botox, *Clin. Med. 4*, 258−261.
17. Li, B., Qian, X., Sarkar, H. K., and Singh, B. R. (1998) Molecular characterization of type E Clostridium botulinum and comparison to other types of Clostridium botulinum, *Biochim. Biophys. Acta 1395*, 21−7.
18. Sharma, S., and Singh, B. R. (2004) Enhancement of the endopeptidase activity of purified neurotoxins A and E by an isolated component of the native neurotoxin associated proteins, *Biochemistry 43*, 4791−4798.
19. Fujinaga, Y., Inoue, K., Watanabe, S., Yokota, K., Hirai, Y., Nagamachi, E., and Oguma, K. (1997) The haemagglutinin of C*lostridium botulinum* type C progenitor toxin plays an essential role in binding of toxin to the epithelial cells of guinea pig small intestine, leading to the efficient absorption of the toxin, *Microbiology 143*, 3841−3847.
20. Fujinaga, Y., Inoue, K., Watanabe, S., Sakaguchi, Y., Arimitsu, H., Lee, J .C., Jin, Y., Matsumura, T., Kabumoto, Y., Watanabe, T., and Ohyama, T. (2004) Molecular characterization of binding subcomponents of C*lostridium botulinum* type C progenitor toxin for intestinal epithelial cells and erythrocytes, *Microbiology 150*, 1529−1538.
21. Arnon, S. S., Schechter, R., Ingelsby, T. V., Henderson, D, A., Bartlett, D. A., Ascher, M. S., Eitzen, E., Fine, A. D., Hauer, J., Layton, M., Lillibridge, S., Osterholm, M. T., O'Toole, T., Parker, G., Perl, T. M., Russell, P. K., Swerdlow, D. L., and Tonat, K. (2001) Botulinum toxin as a biological weapon: medical and public health management, *JAMA 285*, 1059−1070.
22. Shukla, H. D., and Sharma, S. K. (2005) *Clostridium botulinum*: A bug with beauty and weapon, *Crit. Rev. Microbiol. 31*, 11−18.
23. Cai, S., Sarkar, H. K., and Singh, B. R. (1999) Enhancement of the endopeptidase activity of botulinum neurotoxin by its associated proteins and dithiothreitol, *Biochemistry 38*, 6903−6910.
24. Sakaguchi, G. (1983) Clostridium botulinum toxins, *Pharmacol. Ther. 19*, 165−194.
25. Singh, B. R. and Zhang, Z. (2004) Novel proteins within the type E botulinum neurotoxin complex, U.S. Patent No. 6,699,966.
26. Singh, B. R., Li, B., and Read, D. (1995) Botulinum versus tetanus neurotoxins: why is botulinum neurotoxin but not tetanus neurotoxin a food poison?, *Toxicon 33*, 1541−1547.
27. DasGupta, B. R., and Satyamoorthy, V. (1984) Purification and amino acid composition of type A botulinum neurotoxin, *Toxicon 22*, 415−424.
28. Chang, C., Wu, C., and Yang, J. (1978) Circular dichroic analysis of protein conformation: inclusion of β-turns, *Anal. Biochem. 91*, 13−31.
29. Fu, F., Lomneth, R. B., Cai, S., and Singh, B. R. (1998) Role of zinc in the structure and toxic activity of botulinum neurotoxin, *Biochemistry 37*, 5267−5278.
30. Ragone, R., Colonna, G., Bismuto, E., and Irace, G. (1987) Unfolding pathway of myoglobin: effect of denaturants on solvent accessibility to tyrosyl residues detected by second derivative spectroscopy, *Biochemistry 26*, 2130−2134.
31. Singh, B. R., and DasGupta, B. R. (1989) Structure of heavy and light chain subunits of type A botulinum neurotoxin analyzed by circular dichroism and fluorescence measurements, *Mol. Cell. Biochem. 86*, 87−95.
32. Singh, B. R., Foley, J., and Lafontaine, C. (1995) Physicochemical and immunological characterization of type E botulinum neurotoxin binding protein purified from C*lostridium botulinum*, *J. Protein Chem. 14*, 7−18.
33. Raffestien, S., Marvaud, J. C., Cerrato, R., Dupuy, B., and Popoff, M. (2004) Organization and regulation of neurotoxin genes in Clostridium botulinum and Clostridium tetani, *Anaerobe 10*, 93−100.

34. Pace, P. N., Shirley, B. A., and Thompson, J. A. (1989) in *Protein Structure, a Practical Approach* (Chreighton, T. E., Ed.) p 315, IRL Press, New York.
35. Kono, M., Sen, A. C., and Chakravarti, B. (1990) Thermodynamics of thermal and athermal denaturation of gamma-crystallins: changes in conformational stability upon glutathione reaction, *Biochemistry 29*, 464−470.
36. Kukreja, R., and Singh, B. R. (2005) Biologically active novel conformational state of botulinum, the most poisonous poison, *J. Biol. Chem. 280*, 39346−39352.
37. Deshpande, S. S., and Damodaran, S. (1989) Heat-induced conformational changes in phaseolin and its relation to proteolysis, *Biochim. Biophys. Acta*, *998*, 179−188.
38. Li, L., and Singh, B. R. (2000) Role of zinc binding in type A botulinum neurotoxin light chain's toxic structure, *Biochemistry 39*, 10581−10586.
39. Li, L., and Singh, B. R. (2000) Spectroscopic analysis of pH-Induced changes in the molecular features of type A botulinum neurotoxin light chain, *Biochemistry 39*, 6646−6474.
40. Singh, B. R., and DasGupta, B. R. (1990) Conformational changes associated with the nicking and activation of botulinum neurotoxin type E, *Biophys. Chem. 38*, 123−130.
41. Ragone, R., Colonna, G., Balestrieri, C., Servillo, L., and Irace, G. (1984) Determination of Tyrosine exposure in proteins by Second-Derivative Spectroscopy, *Biochemistry 23*, 1871−1875.
42. Singh, B. R., Wasacz, F. M., Strand, S., Jacobsen, R. J., and DasGupta, B. R. (1990) Structural Analysis of Botulinum Neurotoxin type A and E in aqueous and nonpolar solvents by Fourier Transform Infrared, Second Derivative UV Absorption, and Circular Dichroic Spectroscopies, *J. Protein Chem. 9*, 705−713.
43. Singh, B. R. (2006) Botulinum neurotoxin structure, engineering, and novel cellular trafficking and targeting, *Neurotox. Res. 9*, 73−92.
44. Montecucco, C., and Schiavo, G. (1993) Tetanus and botulinum neurotoxins: a new group of zinc proteases, *Trends Biochem. Sci. 18*, 324−327.
45. Cai, S., and Singh, B. R. (2001) Role of the disulfide cleavage induced molten globule state of type A botulinum neurotoxin in its endopeptidase activity, *Biochemistry 50*, 15327−15333.
46. Fu, F. N., Sharma, S. K., and Singh, B. R. (1998) A protease-resistant novel hemagglutinin purified from type A Clostridium botulinum, *J. Protein Chem. 17*, 53−60.
47. Sharma, S. K., and Singh, B. R. (1998) Hemagglutinin binding mediated protection of botulinum neurotoxin from proteolysis, *J. Nat. Toxins 7*, 239−253.
48. Lacy, D. B., Tepp, W., Cohen, A. C., DasGupta, B. R., and Stevens, R. C. (1998) Crystal structure of botulinum neurotoxin type A and implications for toxicity, *Nat. Struct. Biol. 5*, 898−902.
49. Woody, M. A., and DasGupta, B. R. (1989) Effect of tetranitromethane on the biological activities of botulinum neurotoxin types A, B and E, *Mol. Cell. Biochem.* 85, 159−169.

BI701564F